Two-loop QCD penguin contribution to the width difference in $B_s - \bar{B}_s$ mixing

Marvin Gerlach, Ulrich Nierste, Vladyslav Shtabovenko, and Matthias Steinhauser

Institut für Theoretische Teilchenphysik, Karlsruhe Institute of Technology (KIT)

76128 Karlsruhe, Germany

Abstract

We consider two-loop QCD corrections to the element Γ_{12}^q of the decay matrix in $B_q - \bar{B}_q$ mixing, $q = d, s$, in the leading power of the Heavy Quark Expansion. The calculated contributions involve one current-current and one penguin operator and constitute the next step towards a theory prediction for the width difference $\Delta\Gamma_s$ matching the precise experimental data. We present compact analytic results for all matching coefficients in an expansion in m_c/m_b up to second order. Our new corrections are comparable in size to the current experimental error and slightly increase $\Delta\Gamma_s$.

1 Introduction

In particle collisions B_q mesons, where $q = d, s$ labels the flavour of the light valence quark, are produced as flavour eigenstates. This means that they are either meson or antimeson, with beauty quantum number $B = 1$ or $B = -1$, respectively. Subsequently, this pure B_q or $\bar{B}_q$ state evolves into a quantum-mechanical superposition of B_q and $\bar{B}_q$ following the time evolution of damped oscillations. Two accidental features of the Standard Model (SM) permit the precise study of $B_q - \bar{B}_q$ oscillation in modern experiments: First, the smallness of the element V_{cb} of the Cabibbo-Kobayashi-Maskawa (CKM) matrix implies a large B_q lifetime of around $1.5\,$ps, which makes decay-time dependences experimentally observable. Second, the heaviness of the top quark enhances the $B_q - \bar{B}_q$ mixing box diagram, which governs the $B_q - \bar{B}_q$ mixing amplitude, to a level that the oscillation frequency is in the same ballpark as the B_q lifetime.

$B_q - \bar{B}_q$ mixing is described by the 2×2 matrix $M^q - i\Gamma^q/2$ with the hermitian mass and decay matrices M^q and Γ^q, respectively. Diagonalizing $M^q - i\Gamma^q/2$ leads to a "heavy" (H) and a "light" (L) mass eigenstate which are commonly denoted by B_H^q and B_L^q, respectively, and have masses $M_{H,L}$ and widths $\Gamma_{H,L}$. The oscillation phenomena involve the three quantities $|M_{12}^q|$, $|\Gamma_{12}^q|$ and $\arg(-M_{12}^q/\Gamma_{12}^q)$ which are related to the experimentally accessible quantities

$$
\begin{aligned}
\Delta M_q &= M_H^q - M_L^q, \\
\Delta \Gamma_q &= \Gamma_L^q - \Gamma_H^q, \\
a_{\text{fs}}^q &= \text{Im}\frac{\Gamma_{12}^q}{M_{12}^q},
\end{aligned}
\tag{1}
$$

where the CP asymmetry in flavour-specific decays, a_{fs}^q, is typically measured in semileptonic decays. ΔM_q and $\Delta \Gamma_q$ are related to the elements of the mass and decay matrices as

$$
\Delta M_q \simeq 2|M_{12}^q|, \qquad \frac{\Delta \Gamma_q}{\Delta M_q} = -\text{Re}\frac{\Gamma_{12}^q}{M_{12}^q}.
\tag{2}
$$

In the Standard Model (SM) the phase between $-\Gamma_{12}^q$ and M_{12}^q is small, so that a_{fs}^q is much smaller than $\Delta \Gamma_q/\Delta M_q$ and $\Delta \Gamma_q \simeq 2|\Gamma_{12}^q|$.

M_{12}^q is a $\Delta B = 2$ amplitude probing virtual effects of physics beyond the SM (BSM physics) up to mass scales of several 100 TeV. By contrast, Γ_{12}^q is sensitive to new physics in $\Delta B = 1$ transitions. While Γ_{12}^q probes much lower scales than M_{12}^q, it is instead sensitive to effects of feebly coupled BSM particles which are light enough to be produced in B_q decays. Such particles are predicted in theories addressing the strong CP problem [1,2] or as members of the dark sector, see e.g. Ref. [3] for a baryogenesis mechanism utilising $B_q - \bar{B}_q$ mixing and B_q decays into dark matter.

In this paper we calculate QCD corrections to Γ_{12}^q in the SM needed to better predict both $\Delta \Gamma_q/\Delta M_q$ and a_{fs}^q. Currently, better theory predictions are needed in the case of

$B_s - \bar{B}_s$ mixing to be competitive with the precise experimental values

$$
\begin{aligned}
\Delta M_s^{\mathrm{exp}} &= (17.757 \pm 0.007_{\mathrm{(stat)}} \pm 0.008_{\mathrm{(syst)}}) \ \mathrm{ps}^{-1} \qquad [4] \\
\Delta \Gamma_s^{\mathrm{exp}} &= (0.085 \pm 0.004) \ \mathrm{ps}^{-1}. \qquad [5]
\end{aligned}
\tag{3}
$$

Furthermore, there is steady progress with measurements of $\Delta \Gamma_s$ at LHCb [6], CMS [7], and ATLAS [8].

For the calculation of Γ_{12}^q one employs a special operator product expansion, the Heavy Quark Expansion (HQE), which treats the b quark mass m_b as a hard scale. In this way one expresses Γ_{12}^q as a simultaneous expansion in $\Lambda_{\mathrm{QCD}}/m_b$ and $\alpha_s(m_b)$. Each term of the $1/m_b$ expansion involves perturbative coefficients multiplying hadronic matrix elements of local $\Delta B = 2$ operators. Next-to-leading logarithmic order (NLO) QCD corrections at leading power in $1/m_b$ have been computed in Refs. [9–12]. The $1/m_b$ contribution is known to leading order in α_s [13]. The uncertainty resulting from the truncation of the perturbative series of the currently known SM prediction for $\Delta \Gamma_s$ is larger than the experimental error in Eq. (3), which calls for the calculation of higher-order QCD contributions.

First steps towards next-to-next-to-leading order (NNLO) have been undertaken in Ref. [14] where the fermionic corrections of order $\alpha_s^2 N_f$, where $N_f = 5$ is the number of active quark flavours, have been computed including linear terms in the expansion in m_c/m_b. Note that this calculation cannot be used to obtain a_{fs}^q, which is proportional to m_c^2/m_b^2. In this paper we denote any $\mathcal{O}(\alpha_s)$ contribution to Γ_{12}^q as "NLO", irrespective of the Wilson coefficients involved. This complies with the commonly used notation in connection with higher-order QCD calculations, but differs from the language used in previous papers on Γ_{12}^q, in which the small $\Delta B = 1$ penguin Wilson coefficients C_{3-6} are counted as $\mathcal{O}(\alpha_s)$. In order to match the precision of the experimental value in Eq. (3) one needs the yet unknown complete NNLO corrections proportional to two factors of the current-current Wilson coefficients $C_{1,2}$, while the contributions proportional to $C_{1,2}C_{3-6}$ are only needed at NLO. In Ref. [15] for the first time penguin contributions have been considered beyond LO, presenting the terms proportional to $C_{1,2}C_{3-6}\,\alpha_s N_f$.

In this paper we present the QCD corrections to all penguin contributions proportional to the product of $C_{1,2}$ with one of C_{3-6} in an expansion in

$$
z = \left(\frac{m_c^{\mathrm{OS}}}{m_b^{\mathrm{OS}}} \right)^2,
\tag{4}
$$

where the superscript "OS" refers to the on-shell (or pole) scheme, i.e. two-loop contributions of order $\mathcal{O}(\alpha_s)$. Thus this is a step towards the completion of the NLO prediction of Γ_{12}^q, which is a necessary preparation for NNLO. This calculation is more convenient in the "CMM" operator basis of Ref. [16], which avoids problems in connection to γ_5. We also adopt this basis in the calculation presented in this paper. As a byproduct we reproduce the NLO result for the contribution with two copies of $C_{1,2}$ of Refs. [9–12] (expanded

3

in z) after transforming the $\Delta B = 1$ Wilson coefficients to the CMM basis, which is a powerful check of our calculational set-up.

The paper is organised as follows: Sec. 2 introduces the $\Delta B = 1$ and $\Delta B = 2$ operator bases employed by us, Sec. 3 and Appendix A present the methodology of our calculation, Sec. 4 contains the results, and we conclude in Sec. 5.

2   Preliminaries

The effective $|\Delta B| = 1$ weak Hamiltonian in the CMM operator basis [16] reads:

$$
\mathcal{H}_{\text{eff}}^{|\Delta B|=1} \;\; = \;\; \frac{4G_F}{\sqrt{2}} \left[-\lambda_t^s \Big(\sum_{i=1}^{6} C_i Q_i + C_8 Q_8 \Big) - \lambda_u^s \sum_{i=1}^{2} C_i (Q_i - Q_i^u) \right.
$$

$$
\left. + V_{us}^* V_{cb} \sum_{i=1}^{2} C_i Q_i^{cu} + V_{cs}^* V_{ub} \sum_{i=1}^{2} C_i Q_i^{uc} \right] + \text{h.c.} \,, \tag{5}
$$

where $\lambda_a^s = V_{as}^* V_{ab}$, $a = u,c,t$, contains the CKM matrix elements and $\lambda_t = -\lambda_c - \lambda_u$. For definiteness we specify to $b \to s$ decays relevant for $B_s - \bar{B}_s$ mixing. The corresponding expressions for $B_d - \bar{B}_d$ mixing are trivially found by replacing V_{as} with V_{ad}. G_F is the Fermi constant and the dimension-six $\Delta B = 1$ operators are given by

$$
\begin{aligned}
Q_1^u &= \bar{s}_L \gamma_\mu T^a u_L \, \bar{u}_L \gamma^\mu T^a b_L \,, \\
Q_2^u &= \bar{s}_L \gamma_\mu u_L \, \bar{u}_L \gamma^\mu b_L \,, \\
Q_1^{cu} &= \bar{s}_L \gamma_\mu T^a u_L \, \bar{c}_L \gamma^\mu T^a b_L \,, \\
Q_2^{cu} &= \bar{s}_L \gamma_\mu u_L \, \bar{c}_L \gamma^\mu b_L \,, \\
Q_1^{uc} &= \bar{s}_L \gamma_\mu T^a c_L \, \bar{u}_L \gamma^\mu T^a b_L \,, \\
Q_2^{uc} &= \bar{s}_L \gamma_\mu c_L \, \bar{u}_L \gamma^\mu b_L \,, \\
Q_1 &= \bar{s}_L \gamma_\mu T^a c_L \, \bar{c}_L \gamma^\mu T^a b_L \,, \\
Q_2 &= \bar{s}_L \gamma_\mu c_L \, \bar{c}_L \gamma^\mu b_L \,, \\
Q_3 &= \bar{s}_L \gamma_\mu b_L \sum_q \bar{q} \gamma^\mu q \,, \\
Q_4 &= \bar{s}_L \gamma_\mu T^a b_L \sum_q \bar{q} \gamma^\mu T^a q \,, \\
Q_5 &= \bar{s}_L \gamma_{\mu_1} \gamma_{\mu_2} \gamma_{\mu_3} b_L \sum_q \bar{q} \gamma^{\mu_1} \gamma^{\mu_2} \gamma^{\mu_3} q \,, \\
Q_6 &= \bar{s}_L \gamma_{\mu_1} \gamma_{\mu_2} \gamma_{\mu_3} T^a b_L \sum_q \bar{q} \gamma^{\mu_1} \gamma^{\mu_2} \gamma^{\mu_3} T^a q \,, \\
Q_8 &= \frac{g_s}{16\pi^2} m_b \, \bar{s}_L \sigma^{\mu\nu} T^a b_R \, G_{\mu\nu}^a \,, \tag{6}
\end{aligned}
$$

where $q_L = P_L q$ with $P_L = (1 - \gamma_5)/2$. $Q_1^{(u)}$ and $Q_2^{(u)}$ are the current-current operators describing the W-mediated tree-level decay of the b quark including QCD effects. $Q_3, \ldots, Q_8$ are four-quark penguin operators. We list the operator Q_8 (with $\sigma^{\mu\nu} = i[\gamma^\mu, \gamma^\nu]/2$) for completeness; it does not enter the calculations in this paper. g_s is the strong coupling constant and $G_{\mu\nu}^a$ denotes the gluon field strength tensor. In Eq. (6) the sum over q runs over all five quark fields u, d, s, c or b. For our calculation we also need the following evanescent operators [16]

$$
\begin{aligned}
E_1[Q_1] &= \bar{s}_L \gamma^{\mu_1} \gamma^{\mu_2} \gamma^{\mu_3} T^a c \, \bar{c} \gamma_{\mu_1} \gamma_{\mu_2} \gamma_{\mu_3} T^a b_L - 16 Q_1 \,, \\
E_1[Q_2] &= \bar{s}_L \gamma^{\mu_1} \gamma^{\mu_2} \gamma^{\mu_3} c_i \, \bar{c}_j \gamma_{\mu_1} \gamma_{\mu_2} \gamma_{\mu_3} b_L - 16 Q_2 \,, \\
E_1[Q_5] &= \bar{s}_L \gamma^{\mu_1} \gamma^{\mu_2} \gamma^{\mu_3} \gamma^{\mu_4} \gamma^{\mu_5} b_L \sum_q \bar{q} \gamma_{\mu_1} \gamma_{\mu_2} \gamma_{\mu_3} \gamma_{\mu_4} \gamma_{\mu_5} q_j - 20 Q_5 + 64 Q_3 \,, \\
E_1[Q_6] &= \bar{s}_L \gamma^{\mu_1} \gamma^{\mu_2} \gamma^{\mu_3} \gamma^{\mu_4} \gamma^{\mu_5} T^a b_L \sum_q \bar{q} \gamma_{\mu_1} \gamma_{\mu_2} \gamma_{\mu_3} \gamma_{\mu_4} \gamma_{\mu_5} T^a q - 20 Q_6 + 64 Q_4 \quad (7)
\end{aligned}
$$

and the counterparts of $E_1[Q_{1,2}]$ with one or both c replaced by u. The $\Delta B = 1$ operators in Eqs. (6) and (7) destroy a b and $\bar{s}$ quark while creating a $\bar{b}$ and s quark and thereby describe the transition of a $\bar{B}_s \sim b\bar{s}$ into a $B_s \sim \bar{b}s$ meson. The corresponding Feynman diagrams have incoming b quark and outgoing s quark lines.

Using the Hamiltonian in Eq. (5) the width difference $\Delta\Gamma \approx 2|\Gamma_{12}|$ is obtained from

$$
\Gamma_{12}^s = \frac{1}{2 M_{B_s}} \text{Abs} \langle B_s | i \int \mathrm{d}^4 x \, T \, \mathcal{H}_{\text{eff}}^{\Delta B=1}(x) \mathcal{H}_{\text{eff}}^{\Delta B=1}(0) | \bar{B}_s \rangle \,, \tag{8}
$$

where "Abs" stands for the absorptive part and T is the time ordering operator. Γ_{12}^s encodes the information of the inclusive decay rate into final states common to B_s and $\bar{B}_s$ and Eq. (8) employs the optical theorem to relate Γ_{12}^s to the $\bar{B}_s \to B_s$ forward scattering amplitude.

It is convenient to decompose Γ_{12}^s as [9]

$$
\Gamma_{12}^q = -(\lambda_c^q)^2 \Gamma_{12}^{cc} - 2\lambda_c^q \lambda_u^q \Gamma_{12}^{uc} - (\lambda_u^q)^2 \Gamma_{12}^{uu} \,, \tag{9}
$$

where in the practical calculation the quantities Γ_{12}^{ab} are considered.

The Heavy Quark Expansion (HQE) allows us to express the quantities Γ_{12}^{ab} in Eq. (9) in terms of infrared-safe perturbative coefficients and hadronic matrix elements of $\Delta B = 2$ operators. To leading power in $1/m_b$ one only needs two $\Delta B = 2$ operators, which are conveniently chosen as

$$
\begin{aligned}
Q &= \bar{s}_i \gamma^\mu (1 - \gamma^5) b_i \, \bar{s}_j \gamma_\mu (1 - \gamma^5) b_j \,, \\
\widetilde{Q}_S &= \bar{s}_i (1 - \gamma^5) b_j \, \bar{s}_j (1 - \gamma^5) b_i
\end{aligned} \tag{10}
$$

with colour indices i, j. At intermediate steps of the calculation one also encounters

$$
\widetilde{Q} = \bar{s}_i \gamma^\mu (1 - \gamma^5) b_j \, \bar{s}_j \gamma_\mu (1 - \gamma^5) b_i \,,
$$

$$Q_S \;=\; \bar{s}_i\left(1-\gamma^5\right)b_i\,\bar{s}_j\left(1-\gamma^5\right)b_j\,, \tag{11}$$

and operators with more than two Dirac matrices on both quark lines. Q_S can be traded for Q, $\widetilde{Q}_S$, and an operator R_0 describing $1/m_b$-suppressed contributions to Γ_{12}^s [13],

$$Q_S \;=\; -\widetilde{Q}_S - \frac{1}{2}Q + R_0. \tag{12}$$

By subtracting judiciously constructed linear combinations of Q and $\widetilde{Q}_S$, all additional operators entering the calculation are evanescent, meaning that they vanish in $D = 4$ dimensions. We choose [9, 17]

$$
\begin{aligned}
E_1^{(1)} &= \widetilde{Q} - Q\,,\\
E_2^{(1)} &= \bar{b}_i\gamma^\mu\gamma^\nu\gamma^\rho\,P_L\,s_j\bar{b}_j\gamma_\mu\gamma_\nu\gamma_\rho\,P_L\,s_i - (16-4\epsilon)\widetilde{Q}\,,\\
E_3^{(1)} &= \bar{b}_i\gamma^\mu\gamma^\nu\gamma^\rho\,P_L\,s_i\bar{b}_j\gamma_\mu\gamma_\nu\gamma_\rho\,P_L\,s_j - (16-4\epsilon)Q\,,\\
E_4^{(1)} &= \bar{b}_i\gamma^\mu\gamma^\nu\,P_L\,s_j\bar{b}_j\gamma_\nu\gamma_\mu\,P_L\,s_i + (8-8\epsilon)Q_s\,,\\
E_5^{(1)} &= \bar{b}_i\gamma^\mu\gamma^\nu\,P_L\,s_i\bar{b}_j\gamma_\nu\gamma_\mu\,P_L\,s_j + (8-8\epsilon)\widetilde{Q}_s\,,
\end{aligned}
\tag{13}
$$

with the usual $\epsilon = (4 - D)/2$ of dimensional regularisation. The operators on the RHS are understood to be expressed in terms of the minimal physical basis Q, $\widetilde{Q}_S$, e.g. $\widetilde{Q}$ is to be read as $Q + E_1^{(1)}$ in $E_2^{(1)}$. The choice of the $\mathcal{O}(\epsilon)$ terms in the coefficients affect the expressions of the renormalised coefficients H^{ab}, $\widetilde{H}_S^{ab}$ of Q, $\widetilde{Q}_S$ [18]. That is, their specification is part of the definition of the renormalisation scheme of the operators (along with the $\overline{\text{MS}}$ prescription and the use of anticommuting γ_5). Our definitions in Eq. (13) ensure that the coefficients do not depend on the Fierz arrangement [17, 18], i.e. a four-dimensional Fierz transformation of Q, $\widetilde{Q}_S$ does not change C and $\widetilde{C}_S$.

It is thus possible to write Γ_{12}^{ab} in Eq. (9) as

$$\Gamma_{12}^{ab} \;=\; \frac{G_F^2 m_b^2}{24\pi M_{B_s}}\left[H^{ab}(z)\langle B_s|Q|\bar{B}_s\rangle + \widetilde{H}_S^{ab}(z)\langle B_s|\widetilde{Q}_S|\bar{B}_s\rangle\right] + \dots \tag{14}$$

with z defined in Eq. (4). The ellipses denote higher-order terms in Λ_{QCD}/m_b. The matching coefficients H^{ab} and $\widetilde{H}_S^{ab}$ are related to the functions G^{ab} and G_S^{ab} defined in Refs. [9] via (see, e.g., Eq. (21) of Ref. [12])

$$
\begin{aligned}
H^{ab} &= G^{ab} + \frac{\alpha_2}{2}G_S^{ab}\,,\\
\widetilde{H}_S^{ab} &= G_S^{ab}\,\alpha_1\,,
\end{aligned}
\tag{15}
$$

with

$$\alpha_1 \;=\; 1 + \frac{\alpha_s(\mu_2)}{4\pi}C_F\left(6 + 12\log\frac{\mu_2}{m_b}\right)\,,$$

6

$$\alpha_2 = 1 + \frac{\alpha_s(\mu_2)}{4\pi} C_F \left(\frac{13}{2} + 6 \log \frac{\mu_2}{m_b} \right), \qquad (16)$$

where $C_F = (N_c^2 - 1)/(2N_c)$ with $N_c = 3$ denoting the number of colours. We decompose $H^{ab}(z)$ and $\widetilde{H}_S^{ab}(z)$ as follows

$$
\begin{aligned}
H^{ab}(z) &= H^{(c)\,ab}(z) + H^{(cp)\,ab}(z) + H^{(p)\,ab}(z), \\
\widetilde{H}_S^{ab}(z) &= \widetilde{H}_S^{(c)\,ab}(z) + \widetilde{H}_S^{(cp)\,ab}(z) + \widetilde{H}_S^{(p)\,ab}(z),
\end{aligned}
\qquad (17)
$$

where the superscript "(c)" denotes the contributions with two current-current operators $Q_{1,2}$, while "(cp)" refers to those with one operator $Q_{1,2}$ and one penguin operator Q_{3-6} and "(p)" labels the terms involving two penguin operators. The functions $H^{(cp)\,ab}(z)$ and $\widetilde{H}_S^{(cp)\,ab}(z)$ are the main focus of this paper.

3 Calculation

The Wilson coefficients $H^{ab}(z)$ and $\widetilde{H}_S^{ab}(z)$ encode the short-distance physics and are independent of the external states in the matrix elements in Eqs. (8) and (14). Thus one may replace the mesons by free quarks, i.e. calculate the forward-scattering amplitude

$$b + \bar{s} \to \bar{b} + s$$

in perturbation theory and apply the optical theorem in order to extract the desired absorptive part. By equating Eq. (8) with Eq. (14) one determines $H^{ab}(z)$ and $\widetilde{H}_S^{ab}(z)$. The infrared singularities present in both sides of this matching equation factorise, which makes the desired coefficients meaningful infrared-safe perturbative quantities. The external quarks are on-shell, i.e. we have $p_b^2 = m_b^2$ and may choose $p_s = 0$ since we use $m_s = 0$ and terms proportional to $p_b \cdot p_s$ match onto power-suppressed matrix elements. Thus we must evaluate two-point loop integrals with external momentum $q^2 = m_b^2$. In our calculation we regulate the infrared divergences with a gluon mass which introduces a further mass scale, m_g. We introduce the gluon propagator as

$$\frac{i\delta^{ab} \left(g^{\mu\nu} + \xi \frac{p^\mu p^\nu}{-p^2 - i0} \right)}{m_g^2 - p^2 - i0}. \qquad (18)$$

It is possible to expand the Feynman integrals for $m_g \ll m_b$. We perform this expansion at the level of the master integrals as described below. We further employ an arbitrary QCD gauge parameter ξ and use its cancellation as a check of our calculation.

In the following we describe our methodology for the dominant contribution encoded in $H^{cc}(z)$ and $\widetilde{H}_S^{cc}(z)$. The calculational steps for the CKM-suppressed contributions involving $H^{uc}(z)$ and $\widetilde{H}_S^{uc}(z)$ are the same. Our practical calculation proceeds as follows: We consider the bilocal matrix elements

$$\mathrm{Abs}\langle i \int \mathrm{d}^4x \, T O_i(x) O_j(0) \rangle, \qquad (19)$$
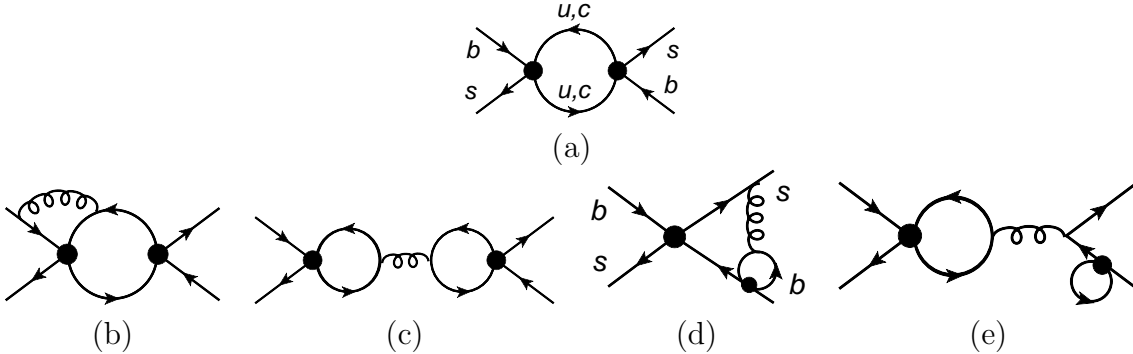
Figure 1: Sample Feynman diagrams contribution to the process $b + \bar{s} \to \bar{b} + s$ with $\Delta B = 1$ operators. The latter are marked by a blob. In (a), (b) and (c) both operators can be from the set $\{Q_1, \ldots, Q_6\}$ whereas in (d) and (e) one of the operators has to be from the set $\{Q_3, \ldots, Q_6\}$.

where O_i and O_j are operators from Eqs. (6) and (7). At one-loop order we have to consider the cases $O_i, O_j \in \{Q_1, \ldots, Q_6\}$ and $O_i \in \{Q_1, \ldots, Q_6\}$, $O_j \in \{E_1^{(1)}, \ldots, E_4^{(1)}\}$. The matrix elements with evanescent operators enter via the renormalisation procedure. One may formulate this procedure in terms of either bare and renormalised Wilson coefficients or bare and renormalised operators. With the former choice we have

$$(C_1, \ldots, C_6, C_{E_1^{(1)}}, \ldots, C_{E_4^{(1)}})^{\text{bare}} = (C_1, \ldots, C_6, *) \begin{pmatrix} Z_{QQ} & Z_{QE} \\ * & * \end{pmatrix} \qquad (20)$$

where Z_{QQ} and Z_{QE} are 6×6 and 6×4 matrices, respectively. They can be extracted from Ref. [19]. The entries in Eq. (20) represented by a $*$ are irrelevant for our calculation. The UV poles contained in Z_{QQ} and Z_{QE} force us to include $\mathcal{O}(\epsilon)$ terms in the one-loop matrix elements $\langle i \int \mathrm{d}^4 x \, T O_i(x) O_j(0) \rangle^{(0)}$ multiplied by Z_{QQ}, Z_{QE}.

At two loops we compute $\langle i \int \mathrm{d}^4 x \, T O_i(x) O_j(0) \rangle$ for $O_i, O_j \in \{Q_1, Q_2\}$, transform the result to the traditional operator basis [20, 21], and compare to the literature [9] in order to have a non-trivial cross check for the implementation of the CMM operator basis. New results are obtained for $\langle i \int \mathrm{d}^4 x \, T Q_{1-2}(x) Q_{3-6}(0) \rangle$.

For our calculation we use a well-tested program chain including `qgraf` [22] for the generation of the amplitudes, `q2e` and `exp` [23, 24] for the identification of the integral families and `FORM` [25] for the algebraic manipulations and the traces of the γ matrices. As an alternative to `q2e` we also use the program `tapir` [26] which automatically generates `FORM` code, in which scalar products in the numerator are re-written in denominator factors and relations implementing a partial fraction decomposition are applied, if necessary. Furthermore, the input files for `FIRE` [27] are automatically generated. The Feynman rules involving the $\Delta B = 1$ and $\Delta B = 2$ operators have been obtained with the help of `FeynRules` [28] and `FeynCalc` [29, 30].

At one-loop order only the type of diagrams shown in Fig. 1(a) contribute. At two

loops we can distinguish four different classes of Feynman diagrams, see also Fig. 1. Figures 1(b) and (c) show the type of diagrams which contribute to the matrix element $\langle i \int d^4 x \, T Q_{1,2}(x) Q_{1,2}(0) \rangle$. These topologies are also present if one of the operators is replaced by a penguin operator. Note that in Fig. 1(c) one of the closed quark loops contains charm or up quarks whereas the other may contain all five active flavours. In Fig. 1(d) and (e) we show sample diagrams which require the presence of a penguin operator. In Fig. 1(d) it is the left operator whereas in (e) it is the one on the external quark line.

We have implemented two approaches for the manipulation of the fermion spinor lines. In the first approach we concentrate on tensor integrals and various manipulations of Dirac structures. We use `FeynCalc` [29–31] together with `Fermat` [32] to obtain formulae for tensor reduction which we then implement in `FORM`. To this end the tensor reduction algorithm of `FeynCalc` was improved using ideas from [33]. In the second approach we construct projectors to all Dirac structures. This has the advantage that we can take traces and afterwards only scalar expressions have to be manipulated. More details can be found in Appendix A.

At this point a comment concerning the expansion in m_c is in order. Since we restrict ourselves to quadratic terms in m_c, i.e. linear terms in z, all loop integrals with both bottom and charm quark lines present in the same loop can be naively Taylor-expanded in m_c before performing the loop integrations.[1] All such diagrams are contained in the class which is represented by Fig. 1(a) and (b). In all other cases we can apply the so-called large-momentum expansion [35] as implemented in `exp` [23, 24]. However, our explicit calculation shows that up to order z indeed a naive expansion in m_c is sufficient.

For the reduction to master integrals we use `FIRE` [27] and `LiteRed` [36, 37]. For all infrared contributions the reduction is performed for general gluon mass m_g. Afterwards we consider the limit of small m_g and perform an asymptotic expansion [35] for $m_g \ll m_b$ at the level of the master integrals. We have performed numerical cross-checks of the expansions with the help of `FIESTA` [38]. After the asymptotic expansion we have to compute single-scale one- and two-loop integrals, most of which are available in the literature (see, e.g., Ref. [35]). The remaining ones are straightforward to compute.

We multiply the matrix element on both sides of the matching equation with Z_ψ^2, where Z_ψ is the quark field renormalisation constant in the $\overline{\text{MS}}$ scheme. This renders both expressions UV-finite. Note, that they still depend on the gauge parameter which is due to the gluon mass used as infrared regulator. For the renormalisation of the charm quark mass we use both the $\overline{\text{MS}}$ and on-shell scheme, see also Section 4. No renormalisation of the bottom or strange quark mass is needed since in the considered order there are no corresponding self-energy diagrams.

For the $\Delta B = 2$ theory we calculate one-loop QCD corrections for the matrix elements

---

[1] There is, however, a $z \log z$ term in one-loop diagrams with a charm mass counterterm. This term does not affect the expansion of the unrenormalised two-loop integrals in z and, moreover, is absent once the result is expressed in terms of $\bar{z} = m_c(m_b)/m_b(m_b)$ [34].
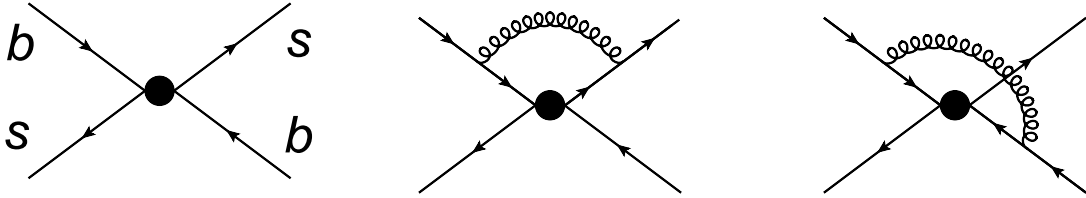
Figure 2: Sample Feynman diagrams with $\Delta B = 2$ operators.

of the minimal operator basis in Eq. (10). Sample Feynman diagrams, which have to be considered at NLO, are shown in Fig. 2. The results of the matrix elements in both the $\Delta B = 1$ and $\Delta B = 2$ theories can be expressed as a linear combination of the tree-level matrix elements of Q, $\widetilde{Q}_S$, R_0 and the unphysical operators in Eq. (13). Since both results are UV-finite we can take the limit $\epsilon \to 0$ and then read off the desired NLO corrections to the $\Delta B = 2$ Wilson coefficients H^{ab} and $\widetilde{H}_S^{ab}$. We observe that the infrared regulator m_g and the gauge parameter cancel from these coefficients, providing a non-trivial check of the calculation. H^{ab} and $\widetilde{H}_S^{ab}$ depend on the renormalisation scales μ_1 and μ_2, at which the renormalised operators are defined in the $\Delta B = 1$ and $\Delta B = 2$ theories, respectively. The μ_1-dependence of H^{ab} and $\widetilde{H}_S^{ab}$ diminishes order-by-order in perturbation theory and is commonly used as a means to estimate the accuracy of the truncated perturbative series. The μ_2-dependence cancels in the matching procedure of the perturbative $\Delta B = 2$ matrix elements with their non-perturbative counterparts.

4 Analytical and numerical results

In the following we discuss the results for the matching coefficients H^{ab} and $\widetilde{H}_S^{ab}(z)$ introduced in Eq. (14).

We start with the analytic expressions for the penguin contributions $H^{(cp)\,ab}(z)$ and $\widetilde{H}_S^{(cp)\,ab}(z)$ (for $ab = uu, uc$ and cc) introduced in Eq. (17). It is convenient to decompose the $\Delta B = 2$ matching coefficients in terms of the $\Delta B = 1$ coefficients C_i of the $|\Delta B| = 1$ Hamiltonian in Eq. (5):

$$
\begin{aligned}
H^{(c)\,ab}(z) &= \sum_{i,j=1}^{2} C_i C_j \, p_{ij}^{ab}(z)\,, \\
\widetilde{H}_S^{(c)\,ab}(z) &= \sum_{i,j=1}^{2} C_i C_j \, p_{ij}^{S,ab}(z)\,, \\
H^{(cp)\,ab}(z) &= \sum_{i=3,...6,8} C_i \left[C_1 p_{1i}^{ab}(z) + C_2 p_{2i}^{ab}(z) \right]\,,
\end{aligned}
$$

$$
\begin{aligned}
\widetilde{H}_S^{(cp)\,ab}(z) &= \sum_{i=3,\ldots6,8} C_i \left[C_1 p_{1i}^{S,ab}(z) + C_2 p_{2i}^{S,ab}(z) \right], \\
H^{(p)\,ab}(z) &= \sum_{i,j=3,\ldots6,8} C_i C_j \, p_{ij}^{ab}(z), \\
\widetilde{H}_S^{(p)\,ab}(z) &= \sum_{i,j=3,\ldots6,8} C_i C_j \, p_{ij}^{S,ab}(z).
\end{aligned}
\tag{21}
$$

We furthermore introduce the perturbative expansion as

$$
p_{ij}^{ab}(z) = p_{ij}^{ab,(0)}(z) + \frac{\alpha_s(\mu_1)}{4\pi} p_{ij}^{ab,(1)}(z) + \mathcal{O}(\alpha_s^2),
\tag{22}
$$

(and analogously for the other coefficients) where $p_{ij}^{ab,(0)}$ refers to one-loop and $p_{ij}^{ab,(1)}$ to two-loop contributions. In this paper the strong coupling constant is defined with five active quark flavours at the renormalisation scale μ_1, i.e. we have $\alpha_s \equiv \alpha_s^{(5)}(\mu_1)$. For later convenience we introduce the squared ratio of the charm and bottom quark masses as

$$
z = \left(\frac{m_c^{\mathrm{OS}}}{m_b^{\mathrm{OS}}} \right)^2 = \left(\frac{\overline{m}_c(m_c)}{\overline{m}_b(m_b)} \right)^2 + \mathcal{O}\left(\alpha_s^2 \right), \qquad\qquad \bar{z} = \left(\frac{\overline{m}_c(m_b)}{\overline{m}_b(m_b)} \right)^2,
\tag{23}
$$

with the $\overline{\mathrm{MS}}$ masses $\overline{m}_q$ and the pole (on-shell) masses m_q^{OS}. While it is easier to employ on-shell masses in the calculation, their poor definition (especially of m_c^{OS}) make them unsuited for numerical evaluations and we will always use $\overline{\mathrm{MS}}$ values as inputs.

The one-loop coefficients $p_{ij}^{ab,(0)}$, $p_{ij}^{S,ab,(0)}$ can be extracted from Ref. [13], where the full m_c dependence has been taken into account, by transforming the result to the operator bases used in this paper. We can reproduce these results in an expansion in z including the linear terms. Note that $p_{i8}^{ab,(0)}$, $p_{i8}^{S,ab,(0)}$ and $p_{88}^{ab,(1)}$, $p_{88}^{S,ab,(1)}$ vanish. For $ab = cc$ the non-zero LO coefficients are

$$
\begin{aligned}
p_{13}^{cc,(0)}(z) &= \sqrt{1-4z}\left(\frac{4}{3} + \frac{8z}{3} \right), & p_{14}^{cc,(0)}(z) &= \sqrt{1-4z}\left(-\frac{5}{36} - \frac{5z}{18} \right), \\
p_{15}^{cc,(0)}(z) &= \sqrt{1-4z}\left(\frac{64}{3} - \frac{160z}{3} \right), & p_{16}^{cc,(0)}(z) &= \sqrt{1-4z}\left(-\frac{20}{9} - \frac{4z}{9} \right), \\
p_{23}^{cc,(0)}(z) &= \sqrt{1-4z}(1 + 2z), & p_{24}^{cc,(0)}(z) &= \sqrt{1-4z}\left(\frac{5}{6} + \frac{5z}{3} \right), \\
p_{25}^{cc,(0)}(z) &= \sqrt{1-4z}(16 - 40z), & p_{26}^{cc,(0)}(z) &= \sqrt{1-4z}\left(\frac{40}{3} + \frac{8z}{3} \right),
\end{aligned}
\tag{24}
$$

as well as

$$
\begin{aligned}
p_{13}^{S,cc,(0)}(z) &= \sqrt{1-4z}\left(-\frac{8}{3} - \frac{16z}{3} \right), & p_{14}^{S,cc,(0)}(z) &= \sqrt{1-4z}\left(-\frac{2}{9} - \frac{4z}{9} \right), \\
p_{15}^{S,cc,(0)}(z) &= \sqrt{1-4z}\left(-\frac{128}{3} - \frac{256z}{3} \right), & p_{16}^{S,cc,(0)}(z) &= \sqrt{1-4z}\left(-\frac{32}{9} - \frac{64z}{9} \right),
\end{aligned}
$$

11

$$p_{23}^{S,cc,(0)}(z) = \sqrt{1-4z}(-2-4z), \qquad\qquad p_{24}^{S,cc,(0)}(z) = \sqrt{1-4z}\left(\frac{4}{3}+\frac{8z}{3}\right),$$

$$p_{25}^{S,cc,(0)}(z) = \sqrt{1-4z}(-32-64z), \qquad\qquad p_{26}^{S,cc,(0)}(z) = \sqrt{1-4z}\left(\frac{64}{3}+\frac{128z}{3}\right).$$

$$(25)$$

The two-loop coefficients $p_{ij}^{ab,(1)}$ are new and are given by

$$p_{13}^{cc,(1)}(z) = \left(\frac{47}{18}-4z\right)L_1 + \frac{56}{9}L_2 + \frac{320z}{9} + \frac{1523}{108} - \frac{5\pi}{18\sqrt{3}},$$

$$p_{14}^{cc,(1)}(z) = \left(-\frac{371}{108}+\frac{5N_H}{54}+\frac{5N_L}{27}+\frac{5N_V}{27}+\frac{59z}{3}\right)L_1 + \frac{1}{54}L_2$$
$$+ \left(\frac{4265}{108}+\frac{5N_L}{9}+\frac{10N_V}{9}+\frac{5\pi^2}{9}\right)z$$
$$- \frac{1649}{162}+\frac{35N_L}{162}+\frac{35N_V}{162}+\frac{5\pi}{108\sqrt{3}}+\frac{5\pi^2}{18}+N_H\left(\frac{85}{162}-\frac{5\pi}{18\sqrt{3}}\right),$$

$$p_{15}^{cc,(1)}(z) = \left(\frac{376}{9}-136z\right)L_1 + \left(\frac{896}{9}-192z\right)L_2 + z\left(-\frac{16408}{9}-768\log(z)\right)$$
$$+ 318 - \frac{40\pi}{9\sqrt{3}},$$

$$p_{16}^{cc,(1)}(z) = \left(-\frac{1484}{27}+\frac{25N_H}{27}+\frac{50N_L}{27}+\frac{50N_V}{27}+\frac{764z}{3}\right)L_1 + \left(\frac{8}{27}+8z\right)L_2$$
$$+ z\left(\frac{22100}{27}+\frac{50N_L}{9}+\frac{100N_V}{9}+\frac{8\pi^2}{9}+32\log(z)\right)$$
$$- \frac{4543}{27}+\frac{130N_L}{81}+\frac{130N_V}{81}+\frac{20\pi}{27\sqrt{3}}+\frac{40\pi^2}{9}+N_H\left(\frac{380}{81}-\frac{25\pi}{9\sqrt{3}}\right),$$

$$p_{23}^{cc,(1)}(z) = \left(-\frac{47}{3}+24z\right)L_1 + \frac{14}{3}L_2 + \frac{170z}{3} + \left(-\frac{677}{18}+\frac{5\pi}{3\sqrt{3}}\right),$$

$$p_{24}^{cc,(1)}(z) = \left(\frac{10}{9}-\frac{5N_H}{9}-\frac{10N_L}{9}-\frac{10N_V}{9}+26z\right)L_1 - \frac{1}{9}L_2$$
$$+ \left(\frac{1729}{18}-\frac{10N_L}{3}-\frac{20N_V}{3}-\frac{10\pi^2}{3}\right)z$$
$$+ \frac{137}{27}-\frac{35N_L}{27}-\frac{35N_V}{27}-\frac{5\pi}{18\sqrt{3}}-\frac{5\pi^2}{3}+N_H\left(-\frac{85}{27}+\frac{5\pi}{3\sqrt{3}}\right),$$

$$p_{25}^{cc,(1)}(z) = \left(-\frac{752}{3}+816z\right)L_1 + \left(\frac{224}{3}-144z\right)L_2 + z\left(\frac{3656}{3}-576\log(z)\right)$$
$$- 580 + \frac{80\pi}{3\sqrt{3}},$$

$$p_{26}^{cc,(1)}(z) = \left(\frac{160}{9}-\frac{50N_H}{9}-\frac{100N_L}{9}-\frac{100N_V}{9}+128z\right)L_1 + \left(-\frac{16}{9}-48z\right)L_2$$

$$+ z \left(\frac{7640}{9} - \frac{100 N_L}{3} - \frac{200 N_V}{3} - \frac{16 \pi^2}{3} - 192 \log(z) \right)$$

$$+ \frac{158}{9} - \frac{260 N_L}{27} - \frac{260 N_V}{27} - \frac{40 \pi}{9 \sqrt{3}} - \frac{80 \pi^2}{3} + N_H \left(-\frac{760}{27} + \frac{50 \pi}{3 \sqrt{3}} \right) \qquad (26)$$

and

$$p_{13}^{S,cc,(1)}(z) = -\frac{4}{3} L_1 - \frac{64}{9} L_2 - \frac{1720 \, z}{9} - \frac{130}{27} - \frac{4 \pi}{9 \sqrt{3}},$$

$$p_{14}^{S,cc,(1)}(z) = \left(\frac{2}{3} + \frac{4 N_H}{27} + \frac{8 N_L}{27} + \frac{8 N_V}{27} \right) L_1 - \frac{16}{27} L_2 + \left(-\frac{40}{27} + \frac{8 N_L}{9} + \frac{16 N_V}{9} + \frac{8 \pi^2}{9} \right) z$$

$$+ \frac{224}{81} + \frac{28 N_L}{81} + \frac{28 N_V}{81} + \frac{2 \pi}{27 \sqrt{3}} + \frac{4 \pi^2}{9} + N_H \left(\frac{68}{81} - \frac{4 \pi}{9 \sqrt{3}} \right),$$

$$p_{15}^{S,cc,(1)}(z) = -\frac{64}{3} L_1 - \frac{1024}{9} L_2 - \frac{27952 z}{9} - \frac{2128}{9} - \frac{64 \pi}{9 \sqrt{3}},$$

$$p_{16}^{S,cc,(1)}(z) = \left(\frac{32}{3} + \frac{40 N_H}{27} + \frac{80 N_L}{27} + \frac{80 N_V}{27} \right) L_1 - \frac{256}{27} L_2$$

$$+ \left(-\frac{1720}{27} + \frac{80 N_L}{9} + \frac{160 N_V}{9} + \frac{128 \pi^2}{9} \right) z$$

$$+ \frac{2344}{27} + \frac{208 N_L}{81} + \frac{208 N_V}{81} + \frac{32 \pi}{27 \sqrt{3}} + \frac{64 \pi^2}{9} + N_H \left(\frac{608}{81} - \frac{40 \pi}{9 \sqrt{3}} \right),$$

$$p_{23}^{S,cc,(1)}(z) = 8 L_1 - \frac{16}{3} L_2 - \frac{448 z}{3} + \frac{116}{9} + \frac{8 \pi}{3 \sqrt{3}},$$

$$p_{24}^{S,cc,(1)}(z) = \left(8 - \frac{8 N_H}{9} - \frac{16 N_L}{9} - \frac{16 N_V}{9} \right) L_1 + \frac{32}{9} L_2$$

$$+ \left(\frac{728}{9} - \frac{16 N_L}{3} - \frac{32 N_V}{3} - \frac{16 \pi^2}{3} \right) z$$

$$+ \frac{632}{27} - \frac{56 N_L}{27} - \frac{56 N_V}{27} - \frac{4 \pi}{9 \sqrt{3}} - \frac{8 \pi^2}{3} + N_H \left(-\frac{136}{27} + \frac{8 \pi}{3 \sqrt{3}} \right),$$

$$p_{25}^{S,cc,(1)}(z) = 128 L_1 - \frac{256}{3} L_2 - \frac{6304 z}{3} + \frac{32}{3} + \frac{128 \pi}{3 \sqrt{3}},$$

$$p_{26}^{S,cc,(1)}(z) = \left(128 - \frac{80 N_H}{9} - \frac{160 N_L}{9} - \frac{160 N_V}{9} \right) L_1 + \frac{512}{9} L_2$$

$$+ \left(\frac{9920}{9} - \frac{160 N_L}{3} - \frac{320 N_V}{3} - \frac{256 \pi^2}{3} \right) z$$

$$+ \frac{2800}{9} - \frac{416 N_L}{27} - \frac{416 N_V}{27} - \frac{64 \pi}{9 \sqrt{3}} - \frac{128 \pi^2}{3} + N_H \left(-\frac{1216}{27} + \frac{80 \pi}{3 \sqrt{3}} \right), \qquad (27)$$

with $L_1 = \log(\mu_1^2/m_b^2)$ and $L_2 = \log(\mu_2^2/m_b^2)$. Furthermore, we introduce the symbols N_L, N_V and N_H which label closed fermion loops with mass 0, m_c and m_b, respectively. In the numerical evaluation we set $N_L = 3$, $N_V = 1$ and $N_H = 1$.

The results for p_{ij}^{uu} and $p_{ij}^{S,uu}$ are obtained from p_{ij}^{cc} and $p_{ij}^{S,cc}$ for $z = 0$. For p_{ij}^{uc} and $p_{ij}^{S,uc}$ we have

$$p_{ij}^{uc,(0)}(z) = \frac{p_{ij}^{cc,(0)}(z) + p_{ij}^{cc,(0)}(0)}{2}, \quad p_{ij}^{S,uc,(0)}(z) = \frac{p_{ij}^{S,cc,(0)}(z) + p_{ij}^{S,cc,(0)}(0)}{2} \, . \tag{28}$$

Since we perform an expansion up to linear order in z, the NLO coefficients $p_{ij}^{uc,(1)}(z)$ can be cast in the following compact form

$$\begin{aligned}
p_{13}^{uc,(1)}(z) &= p_{13}^{cc,(1)}(z/2), \\
p_{14}^{uc,(1)}(z) &= p_{14}^{cc,(1)}(z/2) + \frac{5}{18} z N_V, \\
p_{15}^{uc,(1)}(z) &= p_{15}^{cc,(1)}(z/2) - 384 z \log(2), \\
p_{16}^{uc,(1)}(z) &= p_{16}^{cc,(1)}(z/2) + \frac{25}{9} z N_V + 16 z \log(2), \\
p_{23}^{uc,(1)}(z) &= p_{23}^{cc,(1)}(z/2), \\
p_{24}^{uc,(1)}(z) &= p_{24}^{cc,(1)}(z/2) - \frac{5}{3} z N_V, \\
p_{25}^{uc,(1)}(z) &= p_{25}^{cc,(1)}(z/2) - 288 z \log(2), \\
p_{26}^{uc,(1)}(z) &= p_{26}^{cc,(1)}(z/2) - \frac{50}{3} z N_V - 96 z \log(2),
\end{aligned} \tag{29}$$

as well as

$$\begin{aligned}
p_{13}^{S,uc,(1)}(z) &= p_{13}^{S,cc,(1)}(z/2), \\
p_{14}^{S,uc,(1)}(z) &= p_{14}^{S,cc,(1)}(z/2) + \frac{4}{9} z N_V, \\
p_{15}^{S,uc,(1)}(z) &= p_{15}^{S,cc,(1)}(z/2), \\
p_{16}^{S,uc,(1)}(z) &= p_{16}^{S,cc,(1)}(z/2) + \frac{40}{9} z N_V, \\
p_{23}^{S,uc,(1)}(z) &= p_{23}^{S,cc,(1)}(z/2), \\
p_{24}^{S,uc,(1)}(z) &= p_{24}^{S,cc,(1)}(z/2) - \frac{8}{3} z N_V, \\
p_{25}^{S,uc,(1)}(z) &= p_{25}^{S,cc,(1)}(z/2), \\
p_{26}^{S,uc,(1)}(z) &= p_{26}^{S,cc,(1)}(z/2) - \frac{80}{3} z N_V.
\end{aligned} \tag{30}$$

The expressions in Eqs. (26) to (30) are exact to order z, i.e. they receive corrections of order $z^2 \log z$. Computer-readable expressions of the two-loop coefficients from Eqs. (26), (27), (29) and (30) can be found in the ancillary file to this paper [39]. The two-loop terms proportional to N_L, N_V and N_H have recently been computed in Ref. [15] and we find complete agreement after expanding the exact expression up to linear order in

z and transforming to the operator basis used in [15]. We note that the NLO coefficients with $i = 1, 2$ and $j = 8$ are only one-loop quantities and can be extracted from Ref. [9].

It is interesting to note that the $\sqrt{3}$ in our results originate from the Feynman diagrams in Fig. 1(b) where in one of the closed loops a massive bottom quark is present. We mention that our results passes the checks mentioned above, the gauge parameter and the gluon mass vanish. As an additional check we have re-done the calculation employing dimensional regularisation of the IR divergences, which requires to do the LO matching at order ϵ, and found the same results.

The results in Eqs. (26) to (30) contain terms of order $z \log z$ which result from diagrams with charm self-energies and mass counterterms. The large coefficients of these terms, proportional to the LO term $\gamma_m^{(0)} = 6C_F = 8$ of the mass anomalous dimension, weakens the quality of the perturbative expansion and is especially troublesome for the prediction of a_{fs}^q, from which the z^0 terms cancel. To eliminate these terms one employs the one-loop relation

$$
\begin{aligned}
z &= \bar{z} \left(1 - \gamma_m^{(0)} \frac{\alpha_s(m_b)}{4\pi} \log \bar{z} \right) + \mathcal{O}(\alpha_s^2), \\
p_{ij}^{ab}(z) &= p_{ij}^{ab}(\bar{z}) - \frac{\partial p_{ij}^{ab,(0)}(\bar{z})}{\partial \bar{z}} \frac{\alpha_s(m_b)}{4\pi} \gamma_m^{(0)} \bar{z} \log \bar{z} + \mathcal{O}(\alpha_s^2)
\end{aligned}
\tag{31}
$$

so that trading z for $\bar{z}$ requires the replacement

$$
p_{ij}^{ab,(1)}(z) \;\rightarrow\; \bar{p}_{ij}^{ab,(1)}(\bar{z}) \equiv p_{ij}^{ab,(1)}(\bar{z}) - \frac{\partial p_{ij}^{ab,(0)}(\bar{z})}{\partial \bar{z}} \gamma_m^{(0)} \bar{z} \log \bar{z},
\tag{32}
$$

where $\alpha_s(m_b) = \alpha_s(\mu_1) + \mathcal{O}(\alpha_s^2)$ has been used, and an analogous replacement for $p_{ij}^{S,ab,(1)}(z)$.

The benefit of using $\bar{z}$ instead of z for the quality of the prediction has been demonstrated in Refs. [12, 34] and we refrain from using z in our numerics. This leaves two plausible renormalisation schemes: One may either use $(m_b^{\text{OS}})^2$ or $\bar{m}_b^2(\bar{m}_b)$ in the prefactor of the square bracket of Γ_{12}^{ab} in Eq. (14). The latter choice requires the replacement

$$
\bar{p}_{ij}^{ab,(1)}(\bar{z}) \;\rightarrow\; \bar{\bar{p}}_{ij}^{ab,(1)}(\bar{z}) \equiv \bar{p}_{ij}^{ab,(1)}(\bar{z}) + 8C_F p_{ij}^{ab,(0)}(\bar{z}),
\tag{33}
$$

and an analogous change of $\bar{p}_{ij}^{S,ab,(1)}(\bar{z})$. In Refs. [14, 15] the two mentioned schemes are referred to as "pole" and "$\overline{\text{MS}}$".

Let us next investigate the numerical effects of the new contributions to $H^{ab}(z)$ and $\widetilde{H}_S^{ab}(z)$. For the input values we use $\alpha_s(M_Z) = 0.1179$ [40] and the $\overline{\text{MS}}$ quark masses $m_c(3 \text{ GeV}) = 0.993$ GeV [41] and $m_b(m_b) = 4.163$ GeV [42] which leads $m_c(m_b) = 0.929$ GeV and $\bar{z} \approx 0.0497$. From $m_b(m_b)$ we obtain $m_b^{\text{OS}} = 4.56$ GeV using the one-loop conversion formula. For the computation of the $\Delta B = 1$ matching coefficients we use as matching scale to the Standard Model $\mu_0 = M_W = 80.403$ GeV. The scale μ_1 is set to $m_b(m_b)$.

In the following we discuss the "cc" contribution of the quantities H^{ab} and $\widetilde{H}^{ab}_S$ in the $\overline{\text{MS}}$ scheme. We refrain from showing explicit results for the "uu" and "uc" contributions which show a similar pattern. We have

$$
\begin{aligned}
H^{cc} &= 0.925_{(c)} - 0.051_{(cp)} + (0.002 N_V + 0.002 N_L)_{(p)} \\
&\quad + \frac{\alpha_s}{4\pi}\left[-2.566_{(c)} - 0.696_{(c-gb)} + (-0.846 + 0.0128 N_H + 0.116 N_V + 0.105 N_L)_{(cp)}\right], \\
\widetilde{H}^{cc}_S &= 1.606_{(c)} - 0.084_{(cp)} + (0.002 N_V + 0.002 N_L)_{(p)} \\
&\quad + \frac{\alpha_s}{4\pi}\left[-0.791_{(c)} - 1.114_{(c-gb)} + (-1.363 + 0.021 N_H + 0.186 N_V + 0.168 N_L)_{(cp)}\right],
\end{aligned}
\tag{34}
$$

where "c-gb" refers to the diagrams with two current-current operators and a gluon bridge, see Fig. 1(c). The numerical values are specific to the operator renormalisation scheme chosen by us. The scheme dependence cancels in combination with the NLO Wilson coefficients C_{3-6} entering the numbers label with "cp". From Eq. (34) we observe that at one-loop order the penguin contribution is about a factor 20 smaller than the terms proportional to C_1 and C_2, which justifies to calculate penguin contributions to lower orders in α_s than those with two copies of $C_{1,2}$. However, at two loops the impact of the penguin coefficients is larger. In the case of H^{cc} the relative factor is less than three and in the case of $\widetilde{H}^{cc}_S$ the penguin coefficient is even bigger than the current-current contribution. We want to remark that the numerically most important penguin contribution is the one proportional to C_4.

We want to remark that in all cases the fermionic contributions to the the penguin coefficients, which are known from Ref. [15], are significantly smaller than the non-fermionic terms computed in this paper. Still, using $N_H = N_V = 1$ and $N_L = 3$ we observe a screening of the non-fermionic coefficient of close to 50%.

We observe that the expansion in z is well-behaved. For example, more than 90% of the non-fermionic penguin coefficients at two-loop order in Eq. (34) are provided by the $m_c \to 0$ approximation.

We are now in the position to evaluate the shift of the new corrections to the width difference. To illustrate the numerical effect of the new corrections we omit both the fermionic NNLO contributions computed in [14] and power corrections of order Λ_{QCD}/m_b. We furthermore concentrate on $\Delta\Gamma_s$. In addition to the quark masses and α_s given above we have the following input parameters [43–45]

$$
\begin{aligned}
M_{B_s} &= 5366.88\,\text{MeV}, \\
B_{B_s} &= 0.813 \pm 0.034, \\
\widetilde{B}'_{S,B_s} &= 1.31 \pm 0.09, \\
f_{B_s} &= (0.2307 \pm 0.0013)\,\text{GeV}, \\
\frac{\lambda^s_u}{\lambda^s_t} &= -(0.00865 \pm 0.00042) + (0.01832 \pm 0.00039)i.
\end{aligned}
\tag{35}
$$

16

Correlator	Perturbative order	z-dependence
$O_{1,2} \times O_{1,2}$ [9]	1 loop	exact
$O_{1,2} \times O_{1,2}$ [9]	2 loops	exact
$O_{1,2} \times O_8$ [9]	1 loop	exact
$O_{1,2} \times O_{3-6}$ [9]	1 loop	exact
$O_{1,2} \times O_{3-6}$	2 loops	$\mathcal{O}(z)$
$O_{3-6} \times O_{3-6}$ [13]	1 loop	exact

Table 1: List of ingredients relevant for $\Delta\Gamma_s$. The two-loop result for the $O_{1,2} \times O_{3-6}$ contribution is new.

Let us first consider the quantity $\Delta\Gamma_s$. The contributions entering our prediction are explicitly listed in table 1 Including all known NLO corrections we obtain

$$
\begin{aligned}
\Delta\Gamma_s &= 0.105 \text{ ps}^{-1} + \dots \quad \text{(pole)}, \\
\Delta\Gamma_s &= 0.110 \text{ ps}^{-1} + \dots \quad (\overline{\text{MS}}),
\end{aligned}
\tag{36}
$$

where the ellipses indicate terms of order Λ_{QCD}/m_b. In case the new corrections computed in this paper are excluded we have

$$
\begin{aligned}
\Delta\Gamma_s &= 0.108 \text{ ps}^{-1} + \dots \quad \text{(pole)}, \\
\Delta\Gamma_s &= 0.113 \text{ ps}^{-1} + \dots \quad (\overline{\text{MS}}).
\end{aligned}
\tag{37}
$$

Thus the calculated corrections increase $\Delta\Gamma_s$ by $0.003\,\text{ps}^{-1}$, which is almost as large as today's experimental error in Eq. (3). The size of the correction is also in the ballpark of the hadronic uncertainty, if $\Delta\Gamma_s$ is predicted from $\Delta\Gamma_s/\Delta M_s$, since hadronic uncertainties largely cancel from this ratio [12, 15].

Next, we discuss the relative shift of $\Delta\Gamma_s$ due to the contribution of the penguin contribution in more detail. At one-loop order we obtain

$$
\begin{aligned}
\frac{\Delta\Gamma_s^{p,12\times36,\alpha_s^0}}{\Delta\Gamma_s} &= 7.6\% \quad \text{(pole)}, \\
\frac{\Delta\Gamma_s^{p,12\times36,\alpha_s^0}}{\Delta\Gamma_s} &= 6.1\% \quad (\overline{\text{MS}}),
\end{aligned}
\tag{38}
$$

where the quantity in denominator includes all current-current and current-penguin corrections up to order α_s^1. The penguin-penguin contributions are included up to order α_s^0 (one-loop order). The numerator in Eq. (38) only contains the LO current-penguin contributions (indicated by the superscript "12×36").

At two-loop order we have

$$
\frac{\Delta\Gamma_s^{p,12\times36,\alpha_s}}{\Delta\Gamma_s} = 0.3\% \quad \text{(pole)},
$$

$$\frac{\Delta\Gamma_s^{p,12\times36,\alpha_s}}{\Delta\Gamma_s} \;=\; 1.4\% \quad (\overline{\mathrm{MS}}),$$

(39)

where the numerator contains the new corrections computed in this paper together with the corresponding fermion contributions from [15]. Note that the non-N_f penguin contribution overcompensates the N_f terms [15]. In the pole scheme this leads to tiny corrections below the percent level. In the $\overline{\mathrm{MS}}$ scheme the non-N_f contribution is about a factor three bigger than the N_f terms which leads to a relative correction of -1.4%.

5   Conclusions

In this paper, for the first time, the $\Delta B = 1$ operator basis from Ref. [16] has been used for the computation of NLO corrections to the decay matrix element Γ_{12}^q, governing the width difference between the eigenstates of the $B_q - \bar{B}_q$ mass matrix and the CP asymmetry in semileptonic B_q decays. After reproducing known results [9–11, 14, 15] we have obtained novel two-loop contribution to Γ_{12}^q, namely all contributions involving one current-current operator and one four-quark penguin operator. We have computed these two-loop corrections in an expansion in m_c/m_b including quadratic terms. Computer-readable expressions of our results can be downloaded from [39].

The calculated NLO effects dominate over the previously known partial results which contain only fermion loop contributions. While the NLO penguin contributions are numerically less relevant than those with two large current-current coefficients $C_{1,2}$, they are needed for the theory prediction to match the experimental precision of $\Delta\Gamma_s$ in Eq. (3). To fully keep up with experiment one further needs the contributions involving Q_8 at the two-loop level and a full NNLO (three-loop) calculation of the contributions with two current-current operators. For the NNLO calculation it is instrumental to use the CMM operator basis [16] as we did in this paper.

Acknowledgements

A Projector methodology

In this appendix we briefly describe the approach based on the construction of projectors for the various tensor structures. In general, the scattering amplitude of the process $b + \bar{s} \to \bar{b} + s$ can be parametrized as

$$\mathcal{M} = \sum_{n,m} A^{(n,m)} \, \Gamma^{(n)}_{i_1 i_2 i_3 i_4} \, \Sigma^{(m)}_{c_1 c_2 c_3 c_4} \, \bar{s}^{c_1}_{i_1} b^{c_2}_{i_2} \, \bar{s}^{c_3}_{i_3} b^{c_4}_{i_4} \,, \tag{40}$$

where c_n describe the colour and i_n the spinor indices. Note that the number of colour structures $\Sigma^{(m)}$ is finite. On the other hand, the basis of the Lorentz structure is *a priori* not finite. For a massless s quark the Lorentz structure can be expressed as[2]

$$\Gamma^{(n)}_{i_1 i_2 i_3 i_4} = \left(P_R B^{(n)} \right)_{i_1 i_2} \, \left(P_R B^{(n)} \right)_{i_3 i_4} \equiv \left(P_R B^{(n)} \right) \otimes \left(P_R B^{(n)} \right) \,, \tag{41}$$

where $P_R = (1 + \gamma_5)/2$ and the basis vectors $B^{(n)}$ are given by

$$B^{(0)} = \mathbf{1} \,, \quad B^{(1)} = \gamma_{\mu_1} \,, \quad B^{(2)} = \gamma_{\mu_1} \gamma_{\mu_2} \,, \quad B^{(3)} = \gamma_{\mu_1} \gamma_{\mu_2} \gamma_{\mu_3} \,, \cdots . \tag{42}$$

In four space-time dimensions it is possible to avoid chains with more than four Dirac matrices, which is not possible in $d = 4 - 2\epsilon$ dimensions. However, in a fixed order in the perturbative expansion only a finite number of basis vectors $B^{(n)}$ appear.

In general, the coefficients $A^{(n,m)}$ include dimensionally regularized scalar Feynman integrals. To extract $A^{(n,m)}$ in Eq. (40), one can apply tensor reduction to get scalar integrand expressions. Alternatively, one can make use of the composition of Eq. (40). Hence, we define projection operators for Lorentz ($\mathbf{P}^{(n)}$) and colour space ($\mathbf{C}^{(m)}$), acting as

$$A^{(n,m)} = \mathbf{C}^{(m)} \mathrm{Tr}_d \left[\mathbf{P}^{(n)} \mathcal{M} \right] \,, \tag{43}$$

where $\mathbf{C}^{(m)}$ commutes with the operations applied in Lorentz space. $\mathbf{P}^{(n)}$ is constructed from a linear combination of the structures introduced in Eq. (42). It is understood that the traces are evaluated in d dimensions. Note that in our case no traces including γ_5 appear since Eq. (41) explicitly contains a projector P_R. Thus, Eq. (43) takes the form

$$A^{(n,m)} = \mathbf{C}^{(m)} \sum_i p^{(n,i)} \, \mathrm{Tr}_d \left[\left(B^{(i)} \otimes B^{(i)} \mathcal{M} \right) \right],$$

Using the explicit structure of $\mathcal{M}$ we can express the projector coefficients $p^{(i,j)}$ as the inverse of the Gram matrix, constructed from the tensor basis of Eq. (41)

$$\left(p^{-1} \right)^{(i,j)} = \mathrm{Tr}_d \left[B^{(i)} B^{(j)} \otimes B^{(i)} B^{(j)} \right] \,. \tag{44}$$

Note that on the right-hand side one has a product of two traces.

---

[2]For non-SM interactions or with massive s-quarks the generalization to arbitrary chiralities is straightforward.

A caveat of this approach is that the complexity of the matrix p grows considerably with the number of γ matrices in the basis elements $B^{(n)}$. For our NLO calculation, we have to consider terms up to $n = 9$ which leads to products of two d-dimensional traces where each one contains up to 18 γ-matrices. This non-trivial computational task was done using FORM [25], where the special hints described in the manual have been used. To avoid unnecessary recomputations, we evaluate each occurring trace product separately and include the result in a lookup table.

References

[1] L. Calibbi, F. Goertz, D. Redigolo, R. Ziegler and J. Zupan, Phys. Rev. D **95** (2017) no.9, 095009 [arXiv:1612.08040 [hep-ph]].

[2] J. Martin Camalich, M. Pospelov, P. N. H. Vuong, R. Ziegler and J. Zupan, Phys. Rev. D **102** (2020) no.1, 015023 [arXiv:2002.04623 [hep-ph]].

[3] G. Elor, M. Escudero and A. Nelson, Phys. Rev. D **99** (2019) no.3, 035031 [arXiv:1810.00880 [hep-ph]].

[4] R. Aaij *et al.* [LHCb], JHEP **03** (2021), 137 [arXiv:2011.12041 [hep-ex]].

[5] *Heavy Flavor Averaging Group (HFLAV)*, https://hflav-eos.web.cern.ch/hflav-eos/osc/PDG_2020/\# DMS

[6] R. Aaij *et al.* [LHCb], Eur. Phys. J. C **79** (2019) no.8, 706 [erratum: Eur. Phys. J. C **80** (2020) no.7, 601] [arXiv:1906.08356 [hep-ex]].

[7] A. M. Sirunyan *et al.* [CMS], Phys. Lett. B **816** (2021), 136188 [arXiv:2007.02434 [hep-ex]].

[8] G. Aad *et al.* [ATLAS], Eur. Phys. J. C **81** (2021) no.4, 342 [arXiv:2001.07115 [hep-ex]].

[9] M. Beneke, G. Buchalla, C. Greub, A. Lenz and U. Nierste, Phys. Lett. B **459** (1999), 631-640 [arXiv:hep-ph/9808385 [hep-ph]].

[10] M. Ciuchini, E. Franco, V. Lubicz, F. Mescia and C. Tarantino, JHEP **08** (2003), 031 [arXiv:hep-ph/0308029 [hep-ph]].

[11] M. Beneke, G. Buchalla, A. Lenz and U. Nierste, Phys. Lett. B **576** (2003), 173-183 [arXiv:hep-ph/0307344 [hep-ph]].

[12] A. Lenz and U. Nierste, JHEP **06** (2007), 072 [arXiv:hep-ph/0612167 [hep-ph]].

[13] M. Beneke, G. Buchalla and I. Dunietz, Phys. Rev. D **54** (1996), 4419-4431 [erratum: Phys. Rev. D **83** (2011), 119902] [arXiv:hep-ph/9605259 [hep-ph]].

[14] H. M. Asatrian, A. Hovhannisyan, U. Nierste and A. Yeghiazaryan, JHEP **10** (2017), 191 [arXiv:1709.02160 [hep-ph]].

[15] H. M. Asatrian, H. H. Asatryan, A. Hovhannisyan, U. Nierste, S. Tumasyan and A. Yeghiazaryan, [arXiv:2006.13227 [hep-ph]].

[16] K. G. Chetyrkin, M. Misiak and M. Munz, Nucl. Phys. B **520** (1998), 279-297 [arXiv:hep-ph/9711280 [hep-ph]].

[17] M. Gorbahn, S. Jager, U. Nierste and S. Trine, Phys. Rev. D **84** (2011), 034030 [arXiv:0901.2065 [hep-ph]].

[18] S. Herrlich and U. Nierste, Nucl. Phys. B **455** (1995), 39-58 [arXiv:hep-ph/9412375 [hep-ph]].

[19] P. Gambino, M. Gorbahn and U. Haisch, Nucl. Phys. B **673** (2003), 238-262 [arXiv:hep-ph/0306079 [hep-ph]].

[20] A. J. Buras, M. Jamin, M. E. Lautenbacher and P. H. Weisz, Nucl. Phys. B **400** (1993), 37-74 [arXiv:hep-ph/9211304 [hep-ph]].

[21] G. Buchalla, A. J. Buras and M. E. Lautenbacher, Rev. Mod. Phys. **68** (1996), 1125-1144 [arXiv:hep-ph/9512380 [hep-ph]].

[22] P. Nogueira, J. Comput. Phys. **105** (1993), 279-289

[23] R. Harlander, T. Seidensticker and M. Steinhauser, Phys. Lett. B **426** (1998), 125-132 [arXiv:hep-ph/9712228 [hep-ph]].

[24] T. Seidensticker, [arXiv:hep-ph/9905298 [hep-ph]].

[25] J. Kuipers, T. Ueda, J. A. M. Vermaseren and J. Vollinga, Comput. Phys. Commun. **184** (2013), 1453-1467 [arXiv:1203.6543 [cs.SC]].

[26] F. Herren and M. Gerlach, unpublished.

[27] A. V. Smirnov and F. S. Chuharev, [arXiv:1901.07808 [hep-ph]].

[28] A. Alloul, N. D. Christensen, C. Degrande, C. Duhr and B. Fuks, Comput. Phys. Commun. **185** (2014), 2250-2300 [arXiv:1310.1921 [hep-ph]].

[29] V. Shtabovenko, R. Mertig and F. Orellana, Comput. Phys. Commun. **207** (2016), 432-444 [arXiv:1601.01167 [hep-ph]].

[30] V. Shtabovenko, R. Mertig and F. Orellana, Comput. Phys. Commun. **256** (2020), 107478 [arXiv:2001.04407 [hep-ph]].

[31] R. Mertig, M. Bohm and A. Denner, Comput. Phys. Commun. **64** (1991), 345-359

[32] R. H. Lewis, Computer Algebra System Fermat, `http://www.bway.net/~lewis`.

[33] A. Pak, J. Phys. Conf. Ser. **368** (2012), 012049 [arXiv:1111.0868 [hep-ph]].

[34] M. Beneke, G. Buchalla, C. Greub, A. Lenz and U. Nierste, Nucl. Phys. B **639** (2002), 389-407 [arXiv:hep-ph/0202106 [hep-ph]].

[35] V. A. Smirnov, "Feynman integral calculus," Springer (2006).

[36] R. N. Lee, [arXiv:1212.2685 [hep-ph]].

[37] R. N. Lee, J. Phys. Conf. Ser. **523** (2014), 012059 [arXiv:1310.1145 [hep-ph]].

[38] A. V. Smirnov, Comput. Phys. Commun. **204** (2016), 189-199 [arXiv:1511.03614 [hep-ph]].

[39] `https://www.ttp.kit.edu/preprints/2021/ttp21-015/`.

[40] P. A. Zyla *et al.* [Particle Data Group], PTEP **2020** (2020) no.8, 083C01

[41] K. G. Chetyrkin, J. H. Kühn, A. Maier, P. Maierhofer, P. Marquard, M. Steinhauser and C. Sturm, [arXiv:1710.04249 [hep-ph]].

[42] K. Chetyrkin, J. H. Kühn, A. Maier, P. Maierhofer, P. Marquard, M. Steinhauser and C. Sturm, Theor. Math. Phys. **170** (2012), 217-228 [arXiv:1010.6157 [hep-ph]].

[43] M. Tanabashi *et al.* [Particle Data Group], Phys. Rev. D **98** (2018) no.3, 030001

[44] R. J. Dowdall, C. T. H. Davies, R. R. Horgan, G. P. Lepage, C. J. Monahan, J. Shigemitsu and M. Wingate, Phys. Rev. D **100** (2019) no.9, 094508 [arXiv:1907.01025 [hep-lat]].

[45] A. Bazavov, C. Bernard, N. Brown, C. Detar, A. X. El-Khadra, E. Gámiz, S. Gottlieb, U. M. Heller, J. Komijani and A. S. Kronfeld, *et al.* Phys. Rev. D **98** (2018) no.7, 074512 [arXiv:1712.09262 [hep-lat]].